[redacted]

NASA MEMO 5-18-59L

X 62070339

2/p.

NASA

N63 18042
Code-1

MEMORANDUM

EXPERIMENTAL INVESTIGATION OF FLUTTER OF BUCKLED CURVED PANELS HAVING LONGITUDINAL STRINGERS AT TRANSONIC AND SUPERSONIC SPEEDS

By W. J. Tuovila and Robert W. Hess

Langley Research Center
Langley Field, Va.

CLASSIFICATION CHANGED TO DECLASS.
FIED EFFECTIVE JUNE 12, 1963
AUTHORITY NASA CCN-4 BY J. J. CARR
ARC.

OTS PRICE
XEROX $ 2.60 ph
MICROFILM $ 0.83 mf

[redacted]

NATIONAL AERONAUTICS AND SPACE ADMINISTRATION
WASHINGTON
June 1959

[redacted]

NASA MEMO 5-18-59L

[redacted]

NATIONAL AERONAUTICS AND SPACE ADMINISTRATION

MEMORANDUM 5-18-59L

EXPERIMENTAL INVESTIGATION OF FLUTTER OF BUCKLED CURVED PANELS HAVING LONGITUDINAL STRINGERS AT TRANSONIC AND SUPERSONIC SPEEDS*

By W. J. Tuovila and Robert W. Hess

SUMMARY

18042

Panel-flutter tests have been made at transonic and supersonic speeds with particular reference to buckled curved panels with longitudinal stringers. Other panel configurations were also tested in an attempt to determine effects of skin thickness, curvature, stringers, buckling, pressure differential, and Mach number on the dynamic pressure necessary to start flutter.

For buckled curved panels with longitudinal stringers, the dynamic pressure required to start flutter was increased by increasing the skin thickness and increasing the pressure differential across the panel. There was no apparent effect of Mach number variation from 1.3 to 2.0. None of the curved panels failed because of flutter although the dynamic pressure at the start of flutter was exceeded by a factor of 3 in many cases. The flat panels fluttered at lower dynamic pressures than the curved panels and four flat panels failed because of flutter.

INTRODUCTION

Analytical studies of the panel-flutter problem have been made by many investigators but, as yet, there is no reliable solution for the case of buckled panels of thin-walled cylinders with longitudinal stiffeners. Furthermore, experimental data (refs. 1 to 5) are scarce and, in order to obtain additional data that might be applicable to the flutter of thin-walled stiffened cylinders (simulating missile construction) buckled by axial compression (simulating missile loading), some experiments were performed in the Langley 9- by 18-inch supersonic aeroelasticity

*Title, Unclassified.

[redacted]

[redacted]

tunnel. Cylinders with axial airflow over the outside only were simulated by mounting curved panels as part of the tunnel side wall.

Effects of panel curvature, stiffeners, thickness, buckling, pressure differential, and Mach number were investigated at Mach numbers from 0.85 to 2.0. Most of the testing was done at $M = 1.3$ with buckled curved panels having longitudinal stiffeners.

SYMBOLS

a	speed of sound in test section, ft/sec
E	Young's modulus, psi
l	panel length, in.
M	Mach number
Δp	pressure differential across panel, positive when tunnel static pressure is less than sealing-chamber pressure, psi
q	dynamic pressure, psi
R	radius
t	panel thickness, in.
w	panel width, in.
$\beta = \sqrt{M^2 - 1}$	
ρ	air density, slugs/ft^3

APPARATUS AND TEST METHODS

Models

All the models were made from standard-gage sheet aluminum 2024-T81 alloy having unsupported dimensions of 9.62 inches wide by 11.62 inches long. The nominal skin thicknesses of the models were 0.008 inch, 0.010 inch (measured nearly 0.011 inch), and 0.012 inch.

Figure 1 shows a sketch of the flat and curved stringered panels. The stringers were the same size for both skin thicknesses. They were

[redacted]

glued to the skins but after run 11 flush rivets were added because the glued joints failed when the panels were put under enough compression to produce buckling. The panels were clamped on four edges and buckle depths up to about 1/8 inch were induced by forcing the front and rear clamps toward each other. All four edges of the panels were clamped during the buckling operation. The compression loads were transmitted to the stringers through the skin since the clamps acted only on the skins.

Figure 2 shows a rear view of a curved panel and its instrumentation held in a mounting that is a removable part of the wind-tunnel wall. Not shown in figure 2 is the cylindrical airtight chamber that enclosed the rear of the panel and allowed the pressure behind the panel to be controlled. The vent holes on the right side of figure 2 were used to equalize the pressure in the chamber behind the panels with the test-section static pressure. Figure 3 shows a front view of the same panel prior to a test run.

Instrumentation

The motion of the strip of panel between the upper and middle stringers was detected by six essentially equally spaced inductance coils. The ends of the coils were kept about 0.2 inch away from the panel in order to prevent the panel from contacting the coils during flutter. The strain at the front and rear of the strip of panel below the center stringer was detected by two strain gages glued to the back of the panel. High-speed motion pictures were also taken and a sheet of heat-absorbing glass was used between the photographic lights and the panels to prevent heating the panels. The pressure difference between the test section and the back of the panel was measured with a ±1 psi pressure cell. The signals from the coils, strain gages, and differential pressure cell were recorded by an oscillograph which also recorded the tunnel conditions.

Wind Tunnel

The tests were run in the Langley 9- by 18-inch supersonic aeroelasticity tunnel. It is a two-dimensional blowdown-type tunnel that operates at a maximum stagnation pressure of 95 psia and exhausts into a vacuum vessel. The test-section size is 9 by 18 inches when the $M = 1.3$ and 2.0 nozzles are used and 9 by 14 inches when the slotted transonic nozzle is used.

For the tests of the curved panels at $M = 1.3$ and at transonic speeds, a fairing was extended along the tunnel side wall upstream of the model into the stagnation tank. This fairing was used to prevent tunnel choking and to eliminate shock waves that would be generated by

a ramp type of fairing. Static-pressure measurements made over the area of the panel indicated that the fairing introduced no appreciable gradients over the panel. At $M = 2.0$ a ramp type of fairing was used because reflected shock waves were swept behind the panel and tunnel choking was not a problem. The downstream end of the panels was faired into the side wall.

The vent holes, shown in figure 2, kept the panels at nearly zero pressure differential. By opening a valve on the back of the chamber to either the atmosphere or the tunnel diffuser, the pressure differential could be made positive or negative, respectively. The amount of pressure differential could be controlled by adjusting the valve setting.

Testing Technique

Preliminary to a test, the entire tunnel system up to the valve at the tunnel air-supply tank was evacuated to about 1 psia. The tests were made by manually controlling the opening of the pressure valve to get the desired tunnel conditions. The duration of established flow was 2 to 5 seconds. For the shorter running times the control of the panel pressurization was a matter of presetting the valve on the chamber and taking whatever pressurization resulted. During the longer runs the chamber valve opening was changed during the run in an attempt to control the flutter by changing the panel pressurization. During the relatively short duration of the runs the stagnation temperature remained essentially constant.

RESULTS AND DISCUSSION

The data obtained from these panel tests are presented in table I. In the table there are listed an identifying test run number, the Mach number M, and the speed of sound a. The dynamic pressure q, air density ρ, and pressure differential Δp across the panel are given at the start of flutter (if it occurred), at the maximum value of q of the test run, regardless of whether flutter occurred or not, and when flutter stopped during relatively few test runs. The frequencies listed are, first, the frequency at the start of flutter and, second, any other predominant frequency that appeared during a test run. The panel flutter parameter $\frac{t}{l}\left(\frac{E}{q}\beta\right)^{1/3}$ is given for the start of flutter. Listed under the heading "Remarks" are the following categories: traveling-wave flutter, "oilcanning" oscillation, and no flutter. During traveling-wave flutter a region or regions of maximum deflection moved more or less steadily downstream, much as a flag flutters in the breeze, and no node

lines were present. In contrast, during oilcanning oscillation regions of the panel vibrated in and out as standing waves with node lines of no motion occurring between regions of motion. The traveling-wave flutter and oilcanning oscillation were distinguished primarily by viewing in slow motion the high-speed motion pictures taken during each run. In a number of cases, designated oilcanning oscillation, there was a clean sinusoidal signal near the start of the record, before the flow in the tunnel stabilized, which continued throughout the run. This type of oscillation was attributed to noise, but in cases where the oscillation started after the flow was stabilized it was not possible to distinguish between noise and oilcanning flutter. All the panels tested with the transonic nozzle exhibited an oilcanning type of oscillation, with the exception of two tests. This type of oscillation developed from zero amplitude so gradually that it was difficult to determine the starting point in terms of q. For this reason there are no transonic-flutter results comparable to the Mach 1.3 and Mach 2 data. A sample oscillograph record of a traveling-wave oscillation (run 107) is presented in figure 4(a). Figure 4(b) is a portion of a record (run 164) of an oilcanning oscillation that started from essentially zero amplitude and continued throughout the run.

The various panels are identified by a simple code as follows: The number 8, 10, or 12 indicates the nominal skin thickness in thousandths of an inch; the letter A refers to the material, aluminum alloy; the letter F refers to flat panels or the letter C refers to curved panels; the letter S indicates that the panel had longitudinal stringers; the letter B indicates that the panel was under compression to produce buckling; the letter R indicates that the stringers were restrained by rings. Thus, the designation 10ACSB indicates a curved panel with 0.010-inch-thick aluminum-alloy skin, longitudinal stringers, and in a buckled condition. Most of the testing was done using models 10ACSB and 8ACSB since curved panels with stringers were of primary interest. The test results of these two configurations are plotted, for conditions at the start of flutter, in figure 5 in terms of the panel flutter parameter $\frac{t}{l}\left(\frac{E}{q}\beta\right)^{1/3}$ and $\Delta p/q$. The panel flutter parameter groups the data by Mach number; however, the value of q for flutter was practically the same for $M = 1.3$ and $M = 2$. A conservative value of the flutter parameter for $M = 1.3$ is approximately 0.095 and for $M = 2$ it is approximately 0.13.

The effect of panel pressurization was investigated by making relatively long runs (104 to 109 and 117 to 120) at a value of q high enough to produce flutter. As soon as flutter started the panel pressurization was increased until flutter stopped. Figure 6 shows q plotted against Δp from the start of flutter to the end of flutter for

8ACSB and 10ACSB panels for various tunnel runs at M = 1.3. The results show that positive pressure differentials on the order of 0.5 psi were sufficient to stop the flutter of these panels.

A deep buckle appears to stiffen the panel and raise the flutter dynamic pressure. This is indicated when the results of the 10ACS and 10ACSB panel tests are compared at M = 1.3 in figure 7. The 10ACS panel fluttered at an appreciably lower value of q than did the 10ACSB panel. Although there was no deliberate attempt to form buckles, slight irregularities were present in the 10ACS panels because of fabrication and mounting. A similar trend may be noted in the comparison of the 8ACSB and the 8ACSBR data at M = 2.0. The rings connecting the stringers of the 8ACSBR panel prevented the stringers from moving in torsion and restrained the formation of deep buckles. Consequently the 8ACSB panels had deeper buckles and fluttered at higher values of q. This observation of the significance of the depth of the buckle of a panel clamped on four edges on the flutter dynamic pressure is the same as that made in reference 3.

The effect of curvature and stringers (or aspect ratio) is not easily separated from the effect of buckling. On the basis of the flutter dynamic pressures for panels 10AFSB and 10ACSB at M = 1.3 it appears that, at least for panels with compression buckles, the effect of curvature is favorable (fig. 7). If the results of models 10AC and 10ACS are compared, it would appear that the addition of stringers to unbuckled panels is unfavorable. However, only a few tests were made with unstringered panels and they had high negative pressure differentials which produced buckling during the runs. Because of the stabilizing effect of deep buckles, the 10AC-panel results cannot be compared with the 10ACS-panel results for the effect of stringers only.

The beneficial effect of thickness on the flutter dynamic pressure is demonstrated only for the buckled panels by the difference in the minimum flutter dynamic pressure of the 10ACSB and the 8ACSB panels at M = 1.3. As may be noted in figure 7, for these particular panels the minimum value of q for the 8ACSB panels was approximately half that for the 10ACSB panels.

None of the curved panels failed during flutter although the dynamic pressure at the start of flutter was exceeded by a factor of 3 on many runs. Each run was only 2 to 5 seconds long; however, some panels were run as many as 20 times. Destructive flutter was obtained in four runs (1, 5, 6, and 9) with flat panels. Runs 5 and 9 were made with panels having stringers but the stringers were not fully effective because the bond between stringers and skin failed locally where the buckling occurred. Runs 1 and 6 were made with unstringered panels. It appears, therefore, that panel flutter can be immediately destructive or it can lead to fatigue failure depending on the panel configuration and operating conditions.

It is of interest to superimpose in figure 8 the results of the present tests on figure 14 of reference 3, although the results of reference 3 are for flat panels clamped on four edges with zero pressure differential. The crosshatched areas include all the present test results at $M = 1.3$ and 2.0. The range of the results is attributed to variables affecting panel flutter that are not accounted for in the flutter parameter, such as pressurization and buckle condition. Without stringers the panels had a value of $\frac{w}{l} = 0.83$ and the panels with stringers were assumed to have a value of $\frac{w}{l} = 0.208$ although the long sides were not fully fixed in the instrumented panel section. All the present results fell within or near the flutter boundary of reference 3.

Reference 6 and this report are based on the same experimental program and any differences are due to variations in the interpretation of the data.

CONCLUDING REMARKS

Panel-flutter tests have been made at transonic and supersonic speeds with particular reference to buckled curved panels with longitudinal stringers. The following observations based on these tests can be made:

The results obtained are similar to those found in previous flat-panel tests in that the flutter dynamic pressure of the panels tested was increased with increase in thickness and differential pressure. The curved panels had a higher flutter dynamic pressure than the flat panels.

The effect of Mach number variation from 1.3 to 2.0 on the flutter dynamic pressure was negligible.

There is evidence that deep buckling will increase the flutter dynamic pressure. A panel with small irregularities will have a higher flutter dynamic pressure when the buckle depth is increased by edge compression.

Panel flutter is generally nondestructive and appears to be a problem mainly from the fatigue standpoint; however, destructive flutter is possible.

Langley Research Center,
National Aeronautics and Space Administration,
Langley Field, Va., March 12, 1959.

[redacted]

[redacted]

REFERENCES

1. Sylvester, Maurice A., and Baker, John E.: Some Experimental Studies of Panel Flutter at Mach Number 1.3. NACA TN 3914, 1957. (Supersedes NACA RM L52I16.)

2. Sylvester, Maurice A., Nelson, Herbert C., and Cunningham, Herbert J.: Experimental and Theoretical Studies of Panel Flutter at Mach Numbers 1.2 to 3.0. NACA RM L55E18b, 1955.

3. Sylvester, Maurice A.: Experimental Studies of Flutter of Buckled Rectangular Panels at Mach Numbers From 1.2 to 3.0 Including Effects of Pressure Differential and of Panel Width-Length Ratio. NACA RM L55I30, 1955.

4. Eisley, J. G.: The Flutter of a Two-Dimensional Buckled Plate With Clamped Edges in a Supersonic Flow. OSR-TN-56-296, GALCIT, July 1956.

5. Greenspon, J. E., and Goldman, R. L.: Flutter of Thin Panels at Subsonic and Supersonic Speeds. OSR Tech. Rep. No. 57-65 (ASTIA Doc. No. 136 560), U. S. Air Force, Nov. 1957.

6. Giltner, T. A., and Young, J. P.: Panel Flutter Test Report. Eng. Rep. No. 10,235-M, The Martin Co., Apr. 1958.

[redacted]

TABLE I.- FLUTTER-TEST RESULTS

[Explanation of panel designations: Number 8, 10, or 12 indicates nominal skin thickness in thousandths of an inch; letter A refers to the material, aluminum alloy; letter F refers to flat panels or letter C refers to curved panels; letter S indicates that panel had longitudinal stringers; letter B indicates that panel was under compression to produce buckling; letter R indicates that stringers were restrained by rings]

Run	M	a, ft/sec	Flutter starts			Maximum dynamic pressure			Flutter stops			Frequency, cps	$\frac{t}{l}\left(\frac{E}{q}\beta\right)^{1/3}$	Remarks
			q, psi	ρ, slugs/ft^3	Δp, psi	q, psi	ρ, slugs/ft^3	Δp, psi	q, psi	ρ, slugs/ft^3	Δp, psi			
Panel 10AC														
33	1.3	978	8.4	0.001502	-0.638	17.95	0.00321					160, 200	0.0876	Traveling-wave flutter
35	1.3	978	10.5	.00187	-.90	18.8	.0033	<-1.0				170, 200	.0813	Traveling-wave flutter
36	1.3	978	14.8	.002646	<-1.0	17.9	.0032	-.76				350		Oilcanning oscillation
37	1.3	978	5.5	.00097	-.36	18.3	.00326	<-1.0				118, 270	.1009	Traveling-wave flutter
Panel 10ACB														
38	1.3	978	6.75	0.00120	-0.85	20.4	0.00362	<-1.0				260, 240	0.0943	Traveling-wave flutter
39	1.3	978	13.8	.00244	-.65	15.7	.00278	-.63				370, 375	.0742	Traveling-wave flutter
40	1.3	978	4.6	.00081	-.10	15.5	.00275	-.4				110, 340	.1071	Traveling-wave flutter
41	1.3	978	5.4	.00097	.12	18.3	.00327	-.66				280, 350	.1015	Traveling-wave flutter
Panel 10ACS														
42	1.3	978	8.34	0.00149	-0.76	19.82	0.00354	<-1.0				220, 220	0.0878	Traveling-wave flutter
43	1.3	978				8.7	.00154	-.55						No flutter
44	1.3	978	6.55	.00117	-.18	17.8	.00317	-1.0				375	.0952	Traveling-wave flutter
45	1.3	978	2.5	.00045	-.3	13.8	.00245	<-1.0				120, 255	.1312	Traveling-wave flutter
46	1.3	978	10.8	.00191	0	18.8	.00334	-.98				366, 340		Oilcanning oscillation
47	1.3	978	10.7	.00191	.03	16.60	.00297	-.56				360, 360		Oilcanning oscillation
48	1.3	978	4.2	.00074	.07	20.8	.00369	-1.0				330, 360	.1104	Traveling-wave flutter
49	1.3	978	8.13	.00143	0	8.13	.00143	0				350		Oilcanning oscillation
50	1.3	978	10.25	.00182	-.04	13.3	.00236	0				380		Oilcanning oscillation
51	1.3	978	1.965	.00035	-.195	6.5	.00115	-.29				250		Oilcanning oscillation
52	1.3	978	9.1	.00162	-.01	11.1	.00178	.036						Oilcanning oscillation
Panel 10ACSB														
160	0.85	1,056				8.25	0.00292	-0.22						Oilcanning oscillation
161	.86	1,055				6.79	.00237	-.15						Oilcanning oscillation
162	.86	1,056				10.8	.00378	-.15						Oilcanning oscillation
170	.85	1,056	6.7	0.0024	-0.15	6.7	.0024	-.15						Oilcanning oscillation
172	.85	1,056				6.25	.00235	-.14						Oilcanning oscillation
163	.86	1,055				13.65	.00479	-.13						Oilcanning oscillation
165	.86	1,055				7.4	.0026	-.15						Oilcanning oscillation
166	.86	1,055	6.22	.002185	-.245	11.8	.00418	-.24						Oilcanning oscillation
167	.86	1,055				9	.00314	-.16						Oilcanning oscillation
168	.86	1,055	8.7	.00304	-.22	12.2	.00426	-.19				310, 350		Oilcanning oscillation
169	.86	1,055				8.3	.00291	-.16						Oilcanning oscillation
164	.93	1,044				12	.00408	-.24						Oilcanning oscillation
177	.99	1,033				13.1	.00362	0						Oilcanning oscillation
173	1.0	1,031				5.6	.00151	-.05						Oilcanning oscillation
174	1.0	1,031				10.42	.00283	-.085				290, 390		Oilcanning oscillation
175	1.02	1,028	11.9	.00311	-.13	11.9	.00311	-.13				360		Oilcanning oscillation
176	1.01	1,030				10.7	.00286	-.01						Oilcanning oscillation
180	1.15	1,005				15.3	.00327	.065						Oilcanning oscillation
184	1.15	1,005				18.2	.00392	.27						Oilcanning oscillation
182	1.16	1,003				8.9	.00189	.11						Oilcanning oscillation
183	1.16	1,003				12.7	.00272	.14						Oilcanning oscillation
181	1.15	1,005	7.6	.00141	-.59	17.9	.00386	.17				120	.0960	Traveling-wave flutter
185	1.19	1,000	7.5	.00154	-.25	19.9	.00425	.29				360		Oilcanning oscillation
186	1.23	990	14.1	.00245	-.47	14.1	.00275	-.47				370		Oilcanning oscillation
187	1.25	986	9.3	.00174	-.60	12.7	.00245	-.66						Oilcanning oscillation
188	1.28	983				15.0	.00269	-2.55						Oilcanning oscillation
194	1.30	978				10.5	.00188	-.13						Oilcanning oscillation
189	1.30	978				15.0	.00269	-1.16						Oilcanning oscillation
190	1.31	976				15.6	.00275	-1.2						Oilcanning oscillation
191	1.3	978				17.1	.00305	-1.06						Oilcanning oscillation
193	1.33	971	6.7	.001155	-.66	13.1	.00238	-1.05				200, 700	.0958	Traveling-wave flutter
192	1.33	971				16.4	.00284	-.84						Oilcanning oscillation
197	1.31	976				11.9	.00210	-.39						Oilcanning oscillation
195	1.21	994				17.0	.00340	-1.1						Oilcanning oscillation
196	1.34	976	5.4	.00093	-.52	14.2	.0025	-1.0				350		Oilcanning oscillation

TABLE I.- FLUTTER-TEST RESULTS - Continued

Run	M	a, ft/sec	Flutter starts			Maximum dynamic pressure			Flutter stops			Frequency, cps	$\frac{t}{l}\left(\frac{E}{q}\beta\right)^{1/3}$	Remarks
			q, psi	ρ, slugs/ft³	Δp, psi	q, psi	ρ, slugs/ft³	Δp, psi	q, psi	ρ, slugs/ft³	Δp, psi			
Panel 10ACSB														
178	1.17	1,000				8	0.00167	0.05						Oilcanning oscillation
179	1.17	1,000				12.3	.00258	.11						Oilcanning oscillation
53	1.3	978	10.1	0.00180	-0.12	19.1	.00339	<-1.0				170, 270	0.0824	Traveling-wave flutter
54	1.3	978	6.9	.00123	.06	7	.00127	0	6.8	0.00121	-0.05	300	.0936	Traveling-wave flutter
55	1.3	978	10.73	.0019	-.195	13.08	.00232	-.095				300	.0807	Traveling-wave flutter
56	1.3	978	8.5	.0015	-.09	10.8	.00192	-.08	10.8	.00192	-.08	125	.0873	Traveling-wave flutter
57	1.3	978	9.61	.0017	-.282	15.75	.00281	-.607				200, 300	.0837	Traveling-wave flutter
58	1.3	978				8.72	.00155	.015						No flutter
59	1.3	978	8.3	.00148	-.355	10.95	.00196	-.18				161, 300	.0880	Traveling-wave flutter
60	1.3	978	6.7	.00118	-.05	8.55	.00151	-.03				97, 270	.0945	Traveling-wave flutter
61	1.3	978	7.95	.0014	.18	21.5	.00381	<-1.0				100, 450	.0893	Traveling-wave flutter
62	1.3	978	6.45	.00114	-.016	22.8	.00406	-.28				115, 300	.0957	Traveling-wave flutter
111	1.3	978	9.0	.00160	.13	10.85	.00193	.07				190	.0856	Traveling-wave flutter
112	1.3	978	9.10	.00160	-.115	21.18	.00216	-.17				174, 220	.0853	Traveling-wave flutter
113	1.3	978	8.35	.00148	-.05	9.3	.00169	.075	8.3	.00147	.57	150	.0878	Traveling-wave flutter
114	1.3	978	9.2	.00165	-.15	10.4	.00185	.66				175, 200	.0840	Traveling-wave flutter
115	1.3	978				7.04	.00125	.115						No flutter
116	1.3	978				8.1	.00144	0						No flutter
117	1.3	978	11.7	.00207	-.30	14	.00249	-.14	13.1	.00233	.12	154	.0784	Traveling-wave flutter
118	1.3	978	10.0	.00177	-.05	11.2	.00199	.4	11.2	.00199	.4	134, 110	.0827	Traveling-wave flutter
119	1.3	978	9.4	.00167	-.06	11.9	.00212	.25	11.9	.00212	.25	152, 105	.0839	Traveling-wave flutter
120	1.3	978	9.4	.00167	-.05	11.3	.00200	.10	11.3	.00200	.10	175	.0839	Traveling-wave flutter
121	1.3	978	7.9	.00140	-.02	10.1	.00180	-.03						Oilcanning oscillation
122	2.0	842				11.7	.00118	.02						No flutter
123	2.0	842				18	.00181	.11						No flutter
124	2.0	842	7.63	.00077	-.165	21.3	.00215	.01				150, 450	.115	Traveling-wave flutter
125	2.0	842	7.58	.000768	-.01	20.25	.00205	.245				150	.1153	Traveling-wave flutter
126	2.0	842	8.77	.00088	-.085	23.05	.00218	.14				420	.1098	Traveling-wave flutter
127	2.0	842				11.62	.00117	.01						No flutter
128	2.0	842	9.75	.00098	-.13	12.9	.00130	.025	12.9	.001303	.025	225	.1062	Traveling-wave flutter
129	2.0	842	5.30	.00053	-.10	15.8	.00159	.015				90	.1298	Traveling-wave flutter
130	2.0	842	9.9	.00100	.17	15.9	.00160	.23				450, 500	.1054	Traveling-wave flutter
131	2.0	842	9.1	.00092	.07	15.9	.00160	.18				200	.1084	Traveling-wave flutter
132	2.0	842	8.95	.00090	-.03	12.8	.00129	.025				200, 800	.1090	Traveling-wave flutter
133	2.0	842	6.9	.00069	-.08	16.25	.00164	.045				400, 440	.1190	Traveling-wave flutter
134	2.0	842	8.14	.00082	.03	16.92	.00171	.16				300, 400	.1125	Traveling-wave flutter
135	2.0	842	8.40	.00085	.21	16.9	.00170	.30				350	.1113	Traveling-wave flutter
136	2.0	842	8.05	.00080	.28	19.3	.00196	.47				300, 380	.1130	Traveling-wave flutter
137	2.0	842				13.2	.00133	.40						No flutter
138	2.0	842	8.8	.00088	.31	17.6	.00178	.43				250, 550	.1097	Traveling-wave flutter
139	2.0	842				14	.00135	.15						No flutter
140	2.0	842	8.4	.00085	-.05	14.1	.00142	-.015				400	.1115	Traveling-wave flutter
Panel 10AFSB														
13	1.3	978	2.105	0.00038	-0.205	7.92	0.00140	-0.185	7.74	0.00138	-0.09	270, 450	0.1390	Traveling-wave flutter
14	1.3	978	3.01	.00054	-.135	9.6	.00171	-.095				300, 500	.1233	Traveling-wave flutter
15	1.3	978	9.02	.00161	-.23	14.5	.00233	-.15				400	.0855	Traveling-wave flutter
16	1.3	978	5.13	.00092	-.48	17.2	.00306	-.4				420, 440	.1032	Traveling-wave flutter
17	1.3	978	3.02	.00054	-.01	6.2	.00111	.025				210, 450	.1232	Traveling-wave flutter
Panel 10AF														
1	1.37	970	4.70	0.00081	-----	16.0	0.00268	-------					0.1082	Broke
Panel 10AFS														
2	1.37	970				5.5	0.00095	-------						No flutter
3	1.37	970				11.5	.00192	.6						No flutter
4	1.37	970				12.0	.00201	-.3						No flutter

DECLASSIFIED

TABLE I.- FLUTTER-TEST RESULTS - Continued

Run	M	a, ft/sec	Flutter starts			Maximum dynamic pressure			Flutter stops			Frequency, cps	$\frac{t}{l}\left(\frac{E}{q}\beta\right)^{1/3}$	Remarks
			q, psi	ρ, $\frac{\text{slugs}}{\text{ft}^3}$	Δp, psi	q, psi	ρ, $\frac{\text{slugs}}{\text{ft}^3}$	Δp, psi	q, psi	ρ, $\frac{\text{slugs}}{\text{ft}^3}$	Δp, psi			
Panel 10AFSB														
5	1.31	978	5.8	0.00095	-0.4	10.5	0.00184	<-1.0					0.0990	Broke
Panel 12AF														
10	1.3	980	2:43	0.00043	-0.06	6.35	0.0012	0.06					0.1315	Traveling-wave flutter
11	1.3	980	3.82	.00066	-.12	9.10	.0016	-.07					.1132	Traveling-wave flutter
Panel 8AC														
19	1.3	978	5.9	0.00105	0.016	8.1	0.001362	-0.02				175	0.0788	Traveling-wave flutter
Panel 8ACB														
20	1.3	978	5.7	0.00101	0.02	8.9	0.00159	0.14	8.0	0.00143	0.48	55, 350	0.0797	Traveling-wave flutter
21	1.3	978	2.39	.00042	.08	8.75	.00155	.22				70, 100	.1064	Traveling-wave flutter
22	1.3	978				8.9	.00159	.61						No flutter
Panel 8ACS														
26	1.3	978				8.9	0.00159	0.61						No flutter
27	1.3	978				8.49	.00152	.68						No flutter
63	1.3	978				9.8	.00174	-.02						No flutter
64	1.3	978				7.8	.00138	0						No flutter
65	1.3	978				10.5	.00186	0						No flutter
66	1.3	978				13.5	.0024	0						No flutter
67	1.3	978				14.45	.00256	-.26						No flutter
68	1.3	978				11.6	.00208	-.2						No flutter
85	1.3	978				17.85	.00319	-.55						No flutter
86	1.3	978				12.6	.00224	.09						No flutter
87	1.3	978				12.6	.00224	-.02						No flutter
88	1.3	978				12.87	.00228	-.065						No flutter
89	1.3	978				13.15	.00233	0						No flutter
90	1.3	978	No coil trace			12.6	.0022	-.05						
91	1.3	978	6.08	0.00108	-0.22	10.3	.00183	-.28				250	0.078	Traveling-wave flutter
92	1.3	978	No coil trace			10.8	.00191	-.05						
93	1.3	978				11.0	.00194	-.06						No flutter
94	1.3	978				10.95	.00194	.02						No flutter
95	1.3	978				10.5	.00186	0						No flutter
96	1.3	978				10.55	.00187	-.06						No flutter
28	1.3	978				10.15	.00182	.74						No flutter
29	1.3	978				10.7	.00191	.72						No flutter
30	1.3	978				5.8	.00103	.54						No flutter
31	1.3	978				9.0	.00161	.693						No flutter
32	1.3	978				8.2	.00145	.255						No flutter
Panel 8ACSB														
69	1.3	978				7.6	0.00137	0.15						No flutter
70	1.3	978				12.65	.00224	.03						No flutter
71	1.3	978				10.55	.00187	0						No flutter
72	1.3	978	11.3	0.00202	-0.36	11.3	.00202	-.36	10	0.00178	-0.36	215, 175	0.0634	Traveling-wave flutter
73	1.3	978				8.65	.00153	-.07						No flutter
74	1.3	978				8.7	.00154	.08						No flutter
75	1.3	978				8.4	.00150	.015						No flutter
76	1.3	978				11.3	.00201	-.10						No flutter
77	1.3	978	6.15	.00109	.18	11	.00193	-.14	10.5	.00186	-.06	175, 300	.076	Traveling-wave flutter
78	1.3	978	7.5	.00133	-.24	11.9	.00211	-.36				200, 200	.0726	Traveling-wave flutter
79	1.3	978	8.0	.00141	-.09	10.5	.00186	-.18	10.5	.00186	-.18	200, 150	.0712	Traveling-wave flutter
80	1.3	978				3.4	.00060	0						No flutter

[redacted]

TABLE I.- FLUTTER-TEST RESULTS - Concluded

Run	M	a, ft/sec	Flutter starts			Maximum dynamic pressure			Flutter stops			Frequency, cps	$\frac{t}{l}\left(\frac{E}{q}\beta\right)^{1/3}$	Remarks
			q, psi	ρ, slugs/ft³	Δp, psi	q, psi	ρ, slugs/ft³	Δp, psi	q, psi	ρ, slugs/ft³	Δp, psi			
Panel 8ACSB														
81	1.3	978	4.7	0.00086	0.12	5.2	0.00092	0.10	5.2	0.00092	0.10	165, 250	0.085	Traveling-wave flutter
82	1.3	978	4.4	.00083	.05	4.7	.00092	0				170, 170	.087	Traveling-wave flutter
83	1.3	978				4.3	.00077	0						No flutter
84	1.3	978				5.3	.00093	0						No flutter
97	1.3	978	5.64	.00100	.03	10.28	.00183	-.05				300, 400	.0799	Traveling-wave flutter
98	1.3	978	4.25	.00075	-.035	10.25	.00182	-.215				200, 350	.0878	Traveling-wave flutter
99	1.3	978				10.47	.00186	-.10						No flutter
100	1.3	978	4.47	.00079	.19	17.16	.00305	-.455				300, 500	.0864	Traveling-wave flutter
101	1.3	978				5.25	.00092	0						No flutter
102	1.3	978	4.85	.00086	-.018	5.35	.00095	-.1	5.12	.00091	-.013	200	.0842	Traveling-wave flutter
103	1.3	978	3.45	.00060	.07	10.05	.00181	-.12				400, 300	.0942	Traveling-wave flutter
104	1.3	978	3.95	.00069	-.2	4.00	.0007	-.05	4.00	.0007	-.05	270, 180	.090	Traveling-wave flutter
105	1.3	978	2.7	.00048	-.2	5.1	.0009	0	4.9	.00087	.13	340, 280	.1022	Traveling-wave flutter
106	1.3	978	4.14	.00074	-.14	5.48	.00097	.075	5.14	.00091	.15	300, 350	.0886	Traveling-wave flutter
107	1.3	978	4.03	.00072	-.01	7.55	.00133	.045	7.1	.00126	.155	490, 380	.0894	Traveling-wave flutter
108	1.3	978	4.45	.00079	.07	9.6	.00172	.08	9.45	.00168	.11	320, 500	.094	Traveling-wave flutter
109	1.3	978	5.7	.00102	.11	10.82	.00193	.08	10.5	.00186	.22	350, 300	.080	Traveling-wave flutter
110	1.3	978				10.00	.00177	-.09						No flutter
141	2	842	7.7	.00077	.06	15.4	.00151	.17				500	.0918	Traveling-wave flutter
142	2	842	5.6	.00056	.12	7.3	.00074	.2	7.3	.00074	.2	200, 350	.1021	Traveling-wave flutter
143	2	842	3.4	.00034	-.09	16.05	.0016	-.02				400, 800	.1205	Traveling-wave flutter
144	2	842	4.78	.00047	.01	16.1	.00168	.16				300	.1076	Traveling-wave flutter
145	2	842	3.62	.00036	-.09	12.7	.00128	.04				260, 500	.117	Traveling-wave flutter
146	2	842	3.1	.00031	.035	8.5	.00086	.10	8.5	.00086	.10	100, 500	.1243	Traveling-wave flutter
147	2	842	6.0	.00061	.09	6.0	.00061	.09	5.98	.00060	.02	200	.0998	Traveling-wave flutter
148	2	842	5.6	.00056	.12	7.3	.00074	.20	7.3	.00074	.20	250	.1021	Traveling-wave flutter
149	2	842	4.1	.00042	-.03	7.4	.00076	-.03				300	.1133	Traveling-wave flutter
150	2	842				7.7	.00076	.10						No flutter
151	2	842	4.4	.00042	------	9.1	.00092	-------				270, 440	.1106	Traveling-wave flutter
152	2	842	2.63	.00027	-.05	11.7	.00118	0				250, 350	.1313	Traveling-wave flutter
153	2	842	4.76	.00048	.01	13.9	.0014	.1				340	.1077	Traveling-wave flutter
Panel 8ACSBR														
154	2	842	2.45	0.00025	-0.04	13.7	0.00138	0.065				400, 700	0.1345	Traveling-wave flutter
155	2	842	1.165	.00012	.12	13.73	.00138	.15				300, 450	.1723	Traveling-wave flutter
156	2	842	1.95	.00020	.27	15.5	.00157	.36				280, 600	.1446	Traveling-wave flutter
157	2	842	2.47	.00025	.45	15.4	.00155	.50				300	.1340	Traveling-wave flutter
158	2	842	1.8	.00018	.02	13.8	.00139	.04				300, 600	.1490	Traveling-wave flutter
159	2	842	2.3	.00024	-.04	14.4	.00146	0				300, 600	.1370	Traveling-wave flutter
Panel 8AFS														
7	1.31	978				11.0	0.00195	0.25						No flutter
Panel 8AFSB														
8	1.31	978				13.0	0.00212	<-1.0						No flutter
9	1.31	978	3.36	0.00060	-0.46	19.2	.00113	<-1.0						Broke

[redacted]

DECLASSIFIED

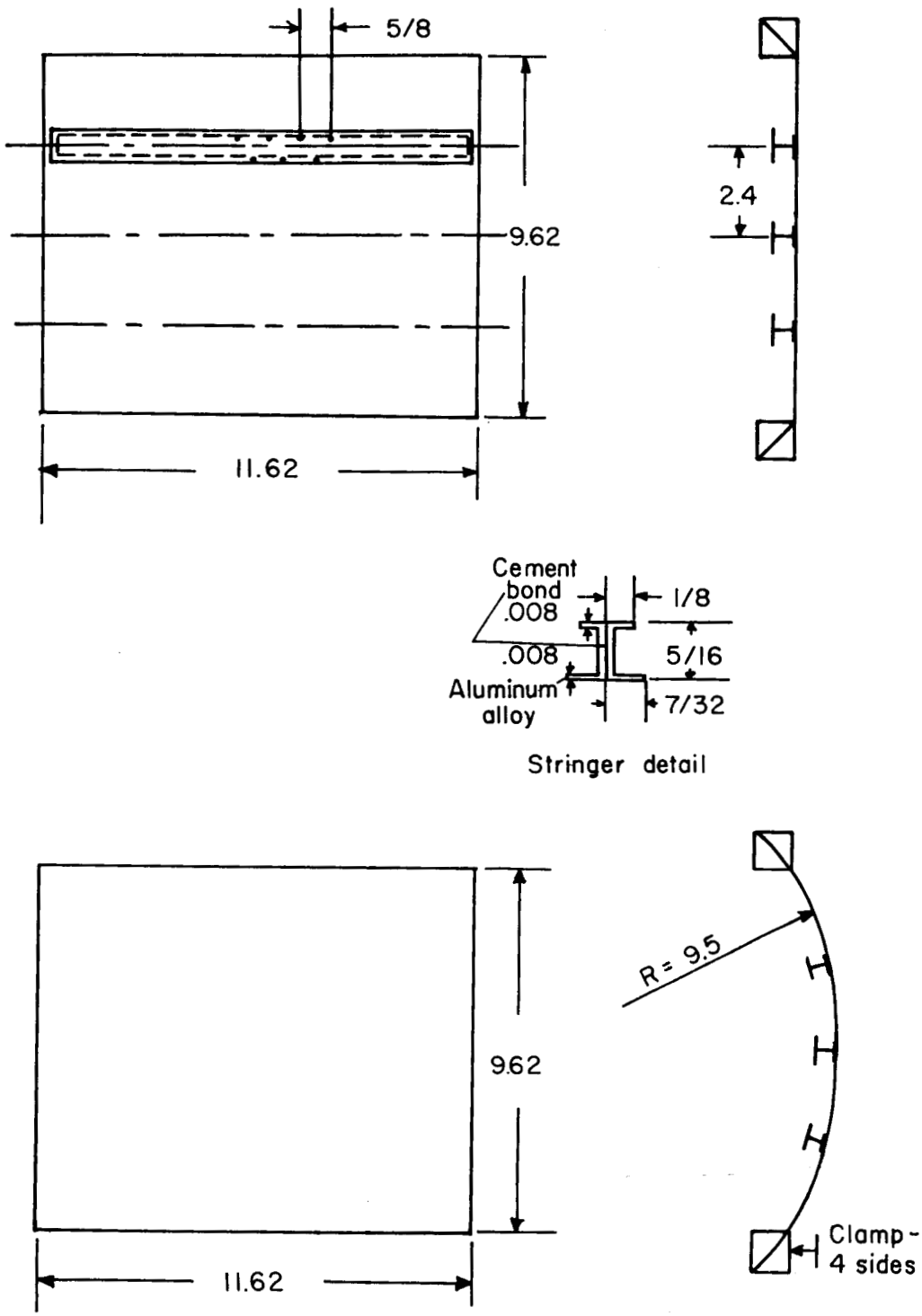
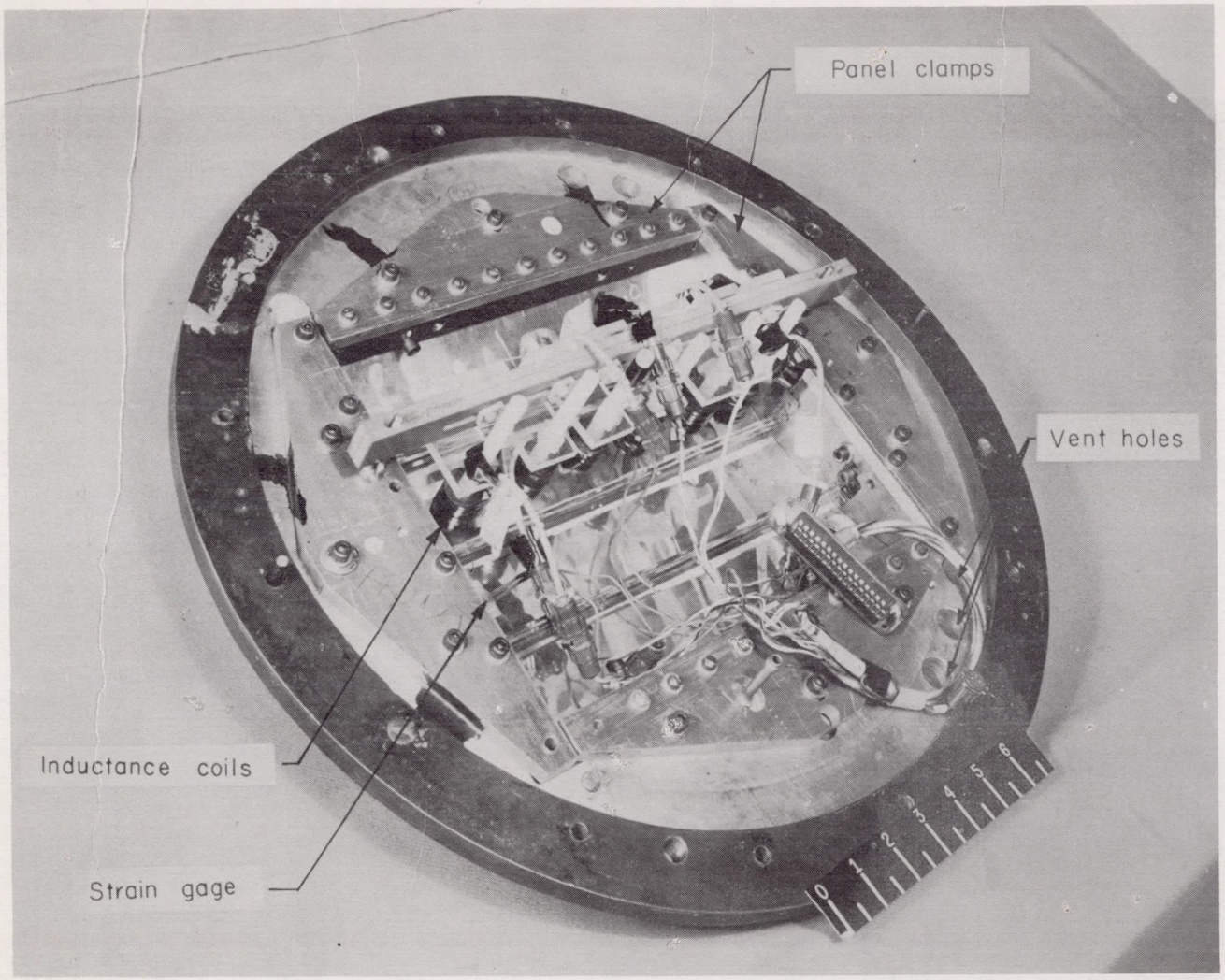
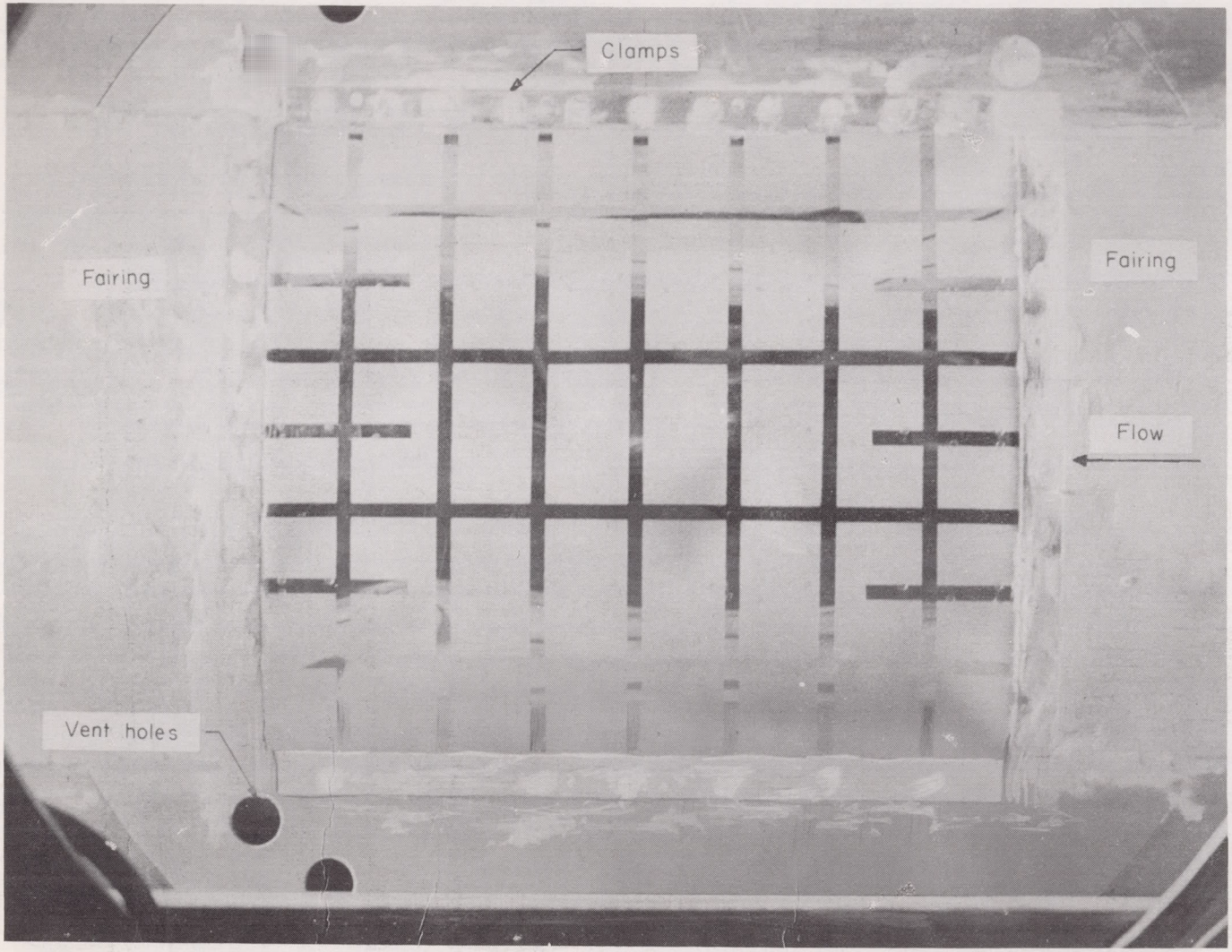


Figure 1.- Sketches of panel configurations. All dimensions are in inches.



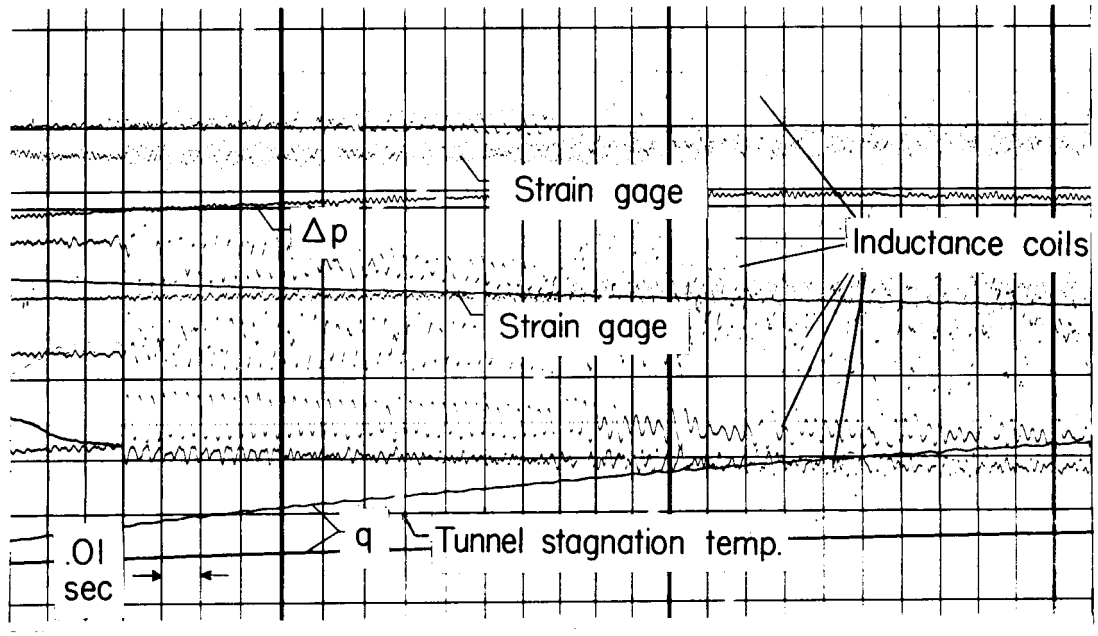
L-58-1414.1

Figure 2.- Rear view of curved panel showing instrumentation.

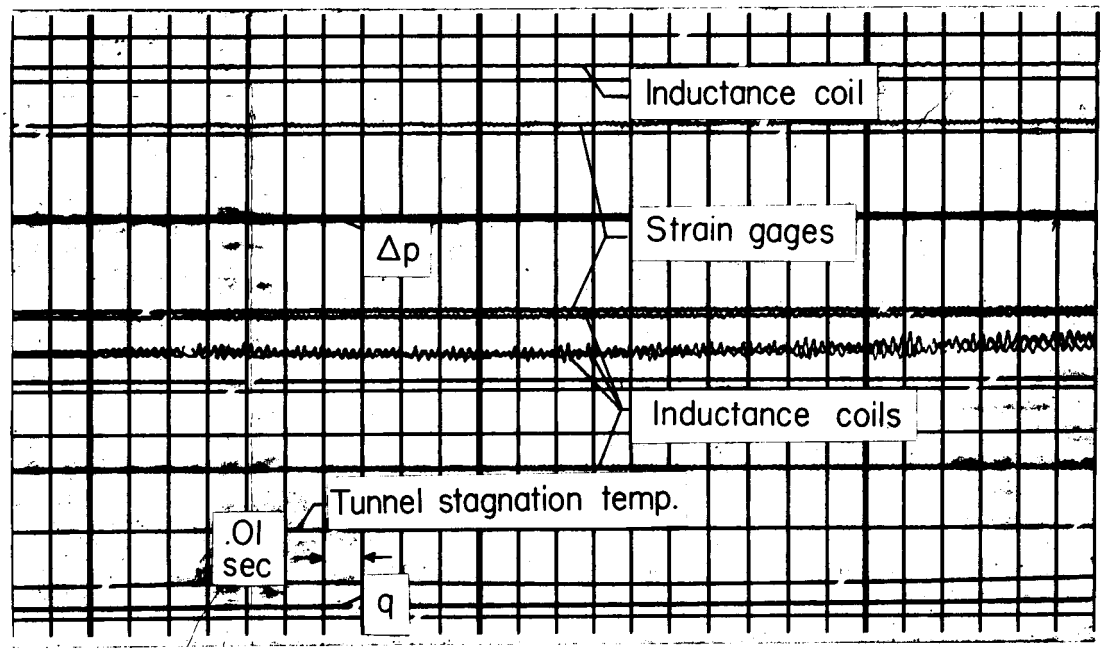


L-59-1889

Figure 3.- Front view of curved panel mounted in tunnel sidewall.



(a) Traveling-wave oscillation at M = 1.3. Run 107; 8ACSB panel.



(b) Oil-canning oscillation at M = 0.93. Run 164; 10ACSB panel.

Figure 4.- Sample oscillograph records for two types of oscillations.

DECLASSIFIED

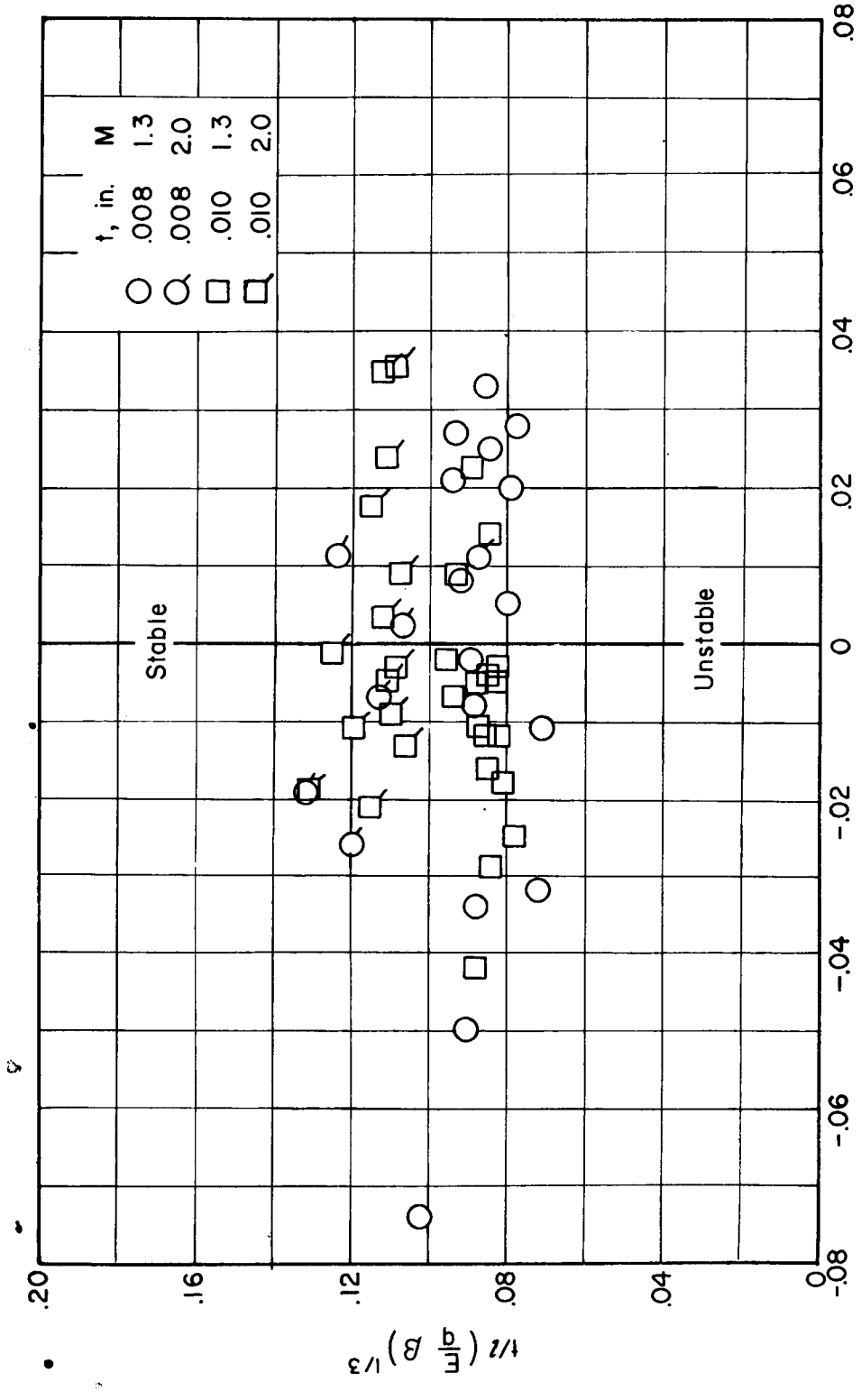


Figure 5.- Flutter boundaries for 8ACSB and 10ACSB panels at M = 1.3 and 2.0.

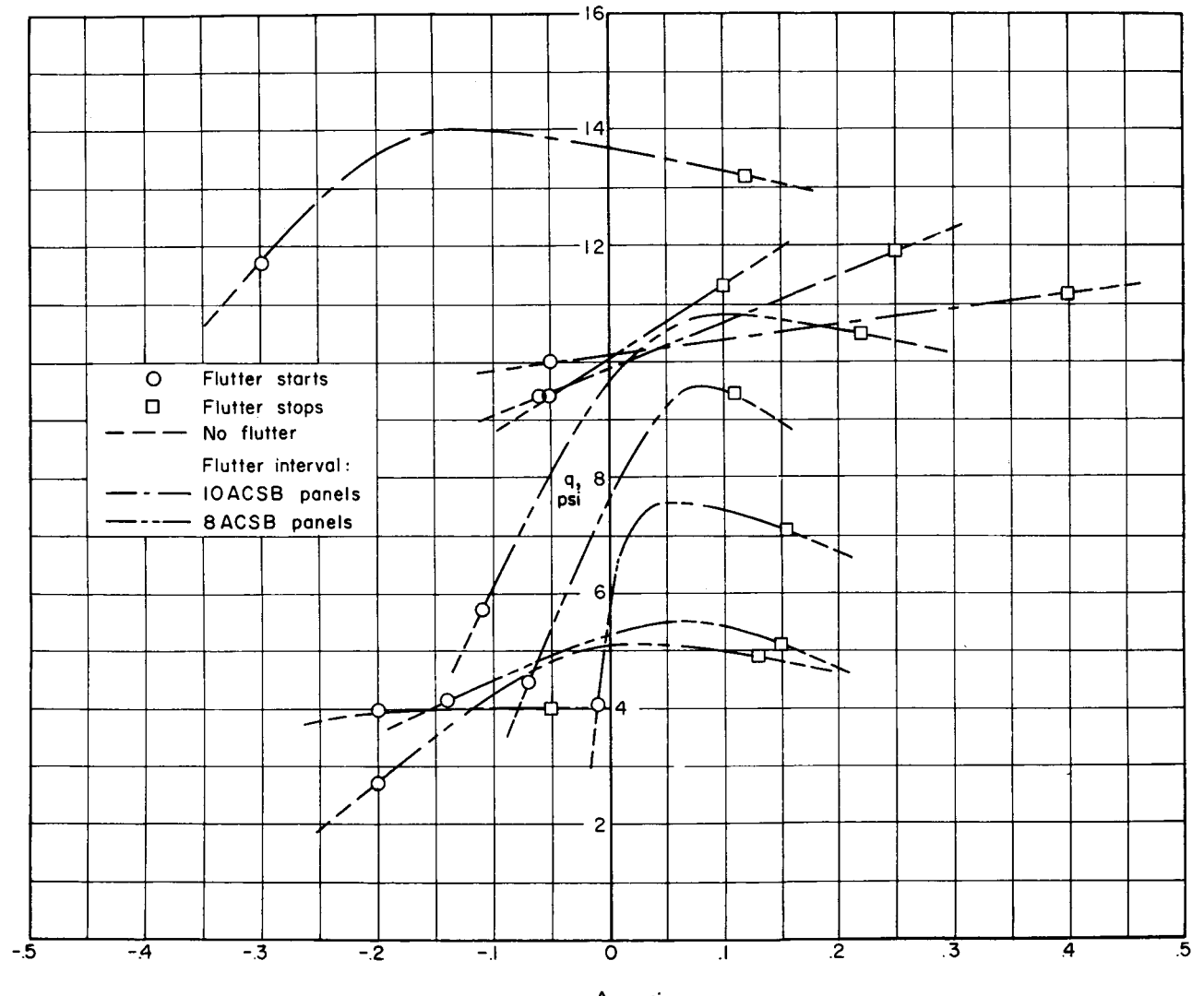


Figure 6.- History of runs where flutter was stopped by increasing Δp. M = 1.3.

DECLASSIFIED

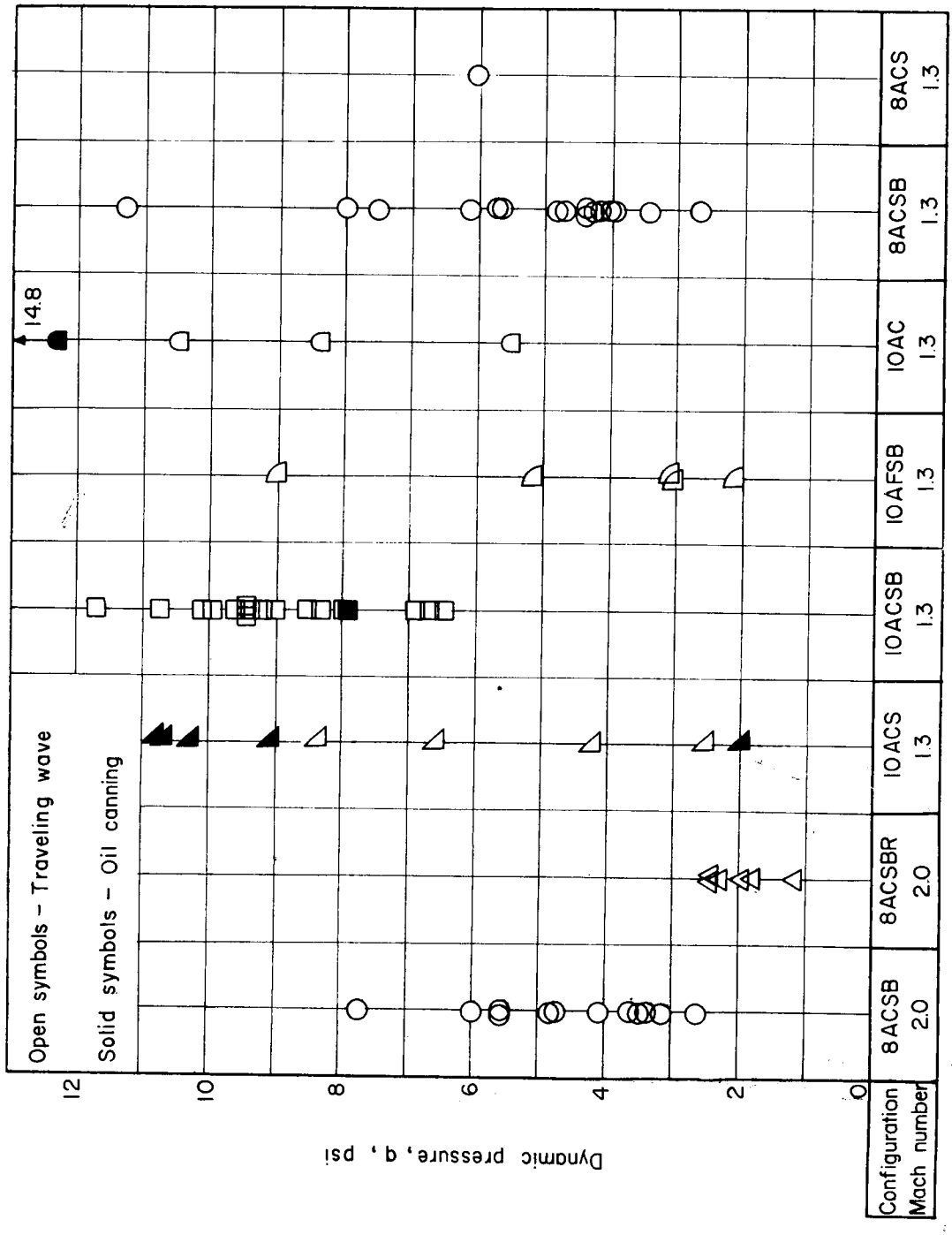


Figure 7.- Comparison of values of dynamic pressure q at start of flutter for different panel configurations.

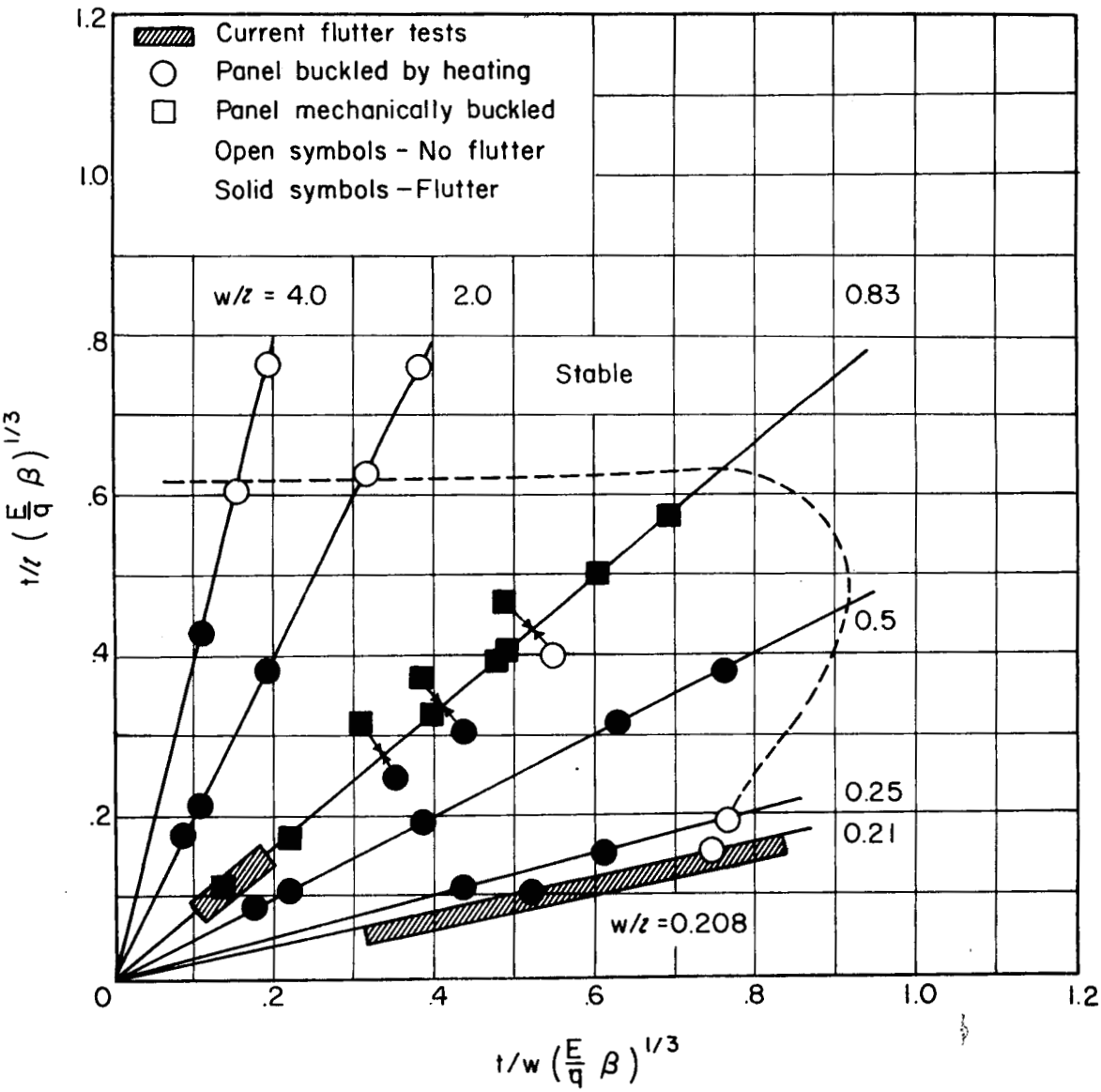


Figure 8.- Current data plotted on figure 14 of reference 3. Mach number for current data varies from M = 1.3 to M = 2.0. Dashed line indicates estimated flutter boundary.

DECLASSIFIED

[redacted]

[redacted]

[redacted]